

Received August 12, 2019, accepted October 3, 2019, date of publication October 8, 2019, date of current version October 22, 2019.

Digital Object Identifier 10.1109/ACCESS.2019.2946285

Hybrid Energy Ratio Allocation Algorithm in a Multi-Base-Station Collaboration System

DONGSHENG HAN¹, SHIJIE LI¹, AND ZHIXIONG CHEN¹

Department of Electronics and Communication Engineering, North China Electric Power University, Beijing 071003, China

Corresponding author: Dongsheng Han (handongsheng@ncepu.edu.cn)

This work was supported in part by the National Natural Science Foundation of China under Grant 61771195 and Grant 61601182, in part by the Natural Science Foundation of Hebei Province under Grant F2018502047 and Grant F2017502059, and in part by the Fundamental Research Funds for Central Universities under Grant 2018MS091.

ABSTRACT Network densification in the 5G system causes a sharp increase in system energy consumption, a development which not only increases operating cost but also carbon emission. With the development of smart power grids, multi-source energy supply and time-of-use (TOU) power price have become effective methods for reducing system energy price (namely, total energy cost). However, the energy generation velocity of renewable energy (RE) is significantly influenced by weather factors. Thus, their energy generation entails large fluctuations, and the system energy allocation strategy involves enormous challenges. Therefore, the energy generation velocity of wind power was combined in a multi-base-station (multi-BS) collaboration system. A multi-BS collaborative energy allocation algorithm called hybrid energy ratio allocation (HERA) algorithm was proposed under RE generation uncertainty. This algorithm can balance the TOU power price of a smart power grid and the energy storage of a BS. The energy supply modes of different energy ratios were adopted following different power prices and energies stored by different BSs, which can effectively mitigate the effect of RE generation fluctuation on the energy allocation strategy of the system. Simulation results indicated that the HERA algorithm can complete the energy ratio allocation of the system and reach the lowest energy cost of BSs.

INDEX TERMS 5G, energy generation uncertainty, energy allocation, energy consumption, energy cost, green communications, multi-base-station collaboration, renewable energy sources.

I. INTRODUCTION

With the rapid development of wireless communication and IoT technologies, the quantity of equipment connected to cellular networks increases significantly. The communication traffic of cellular networks approximately doubles annually. A cellular network will handle 1,000-fold data traffic in the next decade [1]. Network densification can not only solve network under-capacity problems but also effectively reduce system energy consumption. The basic idea is to make base stations (BSs) accessible to served users to improve the densification of access equipment and/or communication links in each served region [2]. However, with the densification of BSs and access equipment, BS energy consumption accounts for an increasingly high proportion in the network. Cellular networks will be confronted with a shortage of spectrum resources and serious channel disturbance. Therefore,

The associate editor coordinating the review of this manuscript and approving it for publication was Ilseun You¹.

improving energy efficiency has become a critical technical index, which must be considered in constructing the next generation of mobile communication systems [3]–[5]. Cell edge users are facing the most critical quality of service (QoS) guarantee problem due to network densification. Multi-BS collaboration can effectively improve the spectrum efficiency of cell edge users [6], [7]. Under considerable quantity of wireless terminals and wireless access networks that must be deployed for the sake of their services, current cellular networks and those that will be deployed in the future, including the incoming 5G, will be faced with massive energy consumption. Such consumption will adversely affect the economy and environment. If no action is taken, then the per capita greenhouse gas emissions of information and communications technology are predicted to reach approximately 130 kg in 2020 [8]. Cellular network consumes approximately 120 TWh of electricity annually. Mobile operators spend approximately USD13 billion yearly in 5 billion connections, thus, the enormous energy demand of cellular

network operators cannot be satisfied only by improving energy efficiency [9]. Therefore, new energies and technologies to handle the exponential growth of energy consumption and carbon emissions of corresponding emerging wireless networks must be developed. In practice, the ever-increasing energy consumption forces network operators to pay huge bills, which only account for half of their operation cost. For cellular network operators, reducing fossil fuel consumption aims at not only realizing green communication for which the natural environment is responsible but also solving the serious economic pressure faced by mobile operators.

With the development of smart power grids, equipping BSs with devices of renewable energy (RE) and using RE or hybrid energy to activate BS systems have become an effective means of solving energy-saving problems and reducing the energy cost of cellular networks [10], [11]. The time-of-use (TOU) power price strategy will be adopted for new-type smart power grids because this strategy can benefit clients and the power grid. The TOU power price strategy can reduce the energy cost of the client (and carbon emission). Conversely, power price is decided by the power grid load, thus confirming that this strategy can reduce peak energy consumption and global energy cost. Smart power grids encourage clients to manage their energy demand, guide them to consume minimal energy during the high-power-price period, or transfer power consumption to non-peak periods to improve energy utilization efficiency and substantially reduce energy cost and carbon emissions [12], [13].

However, generating RE is seriously influenced by the weather and various challenges are posed to the RE supply for BSs given the randomness and fluctuation of the energy generation rate [14], thus, establishing a reasonable energy allocation strategy will be critical for realizing RE supply to BSs. To optimize the energy demand-side management and RE generation model, the authors of [15] decomposed the green energy supply problem into two sub-problems (namely, the minimization problem of weighed energy and the green energy system scale from the angle of green energy supply), moreover, two proposed algorithms for solving the green energy supply optimize the traffic load of the BS, the size of the solar panels, and the capacity of the energy storage device. Ju R et al [16] developed an electric load and power supply model containing random components by the constraint conditions of power supply reliability and equipment quantity, a multi-objective optimization algorithm is proposed to optimize the configuration of the wind-solar hybrid energy supply system. The authors of [17] suggested a new noncooperative game model, using an M/M/1 inventory queue model, considered RE supply status, investigated the influence of the energy supply and storage/inventory level of RE suppliers on QoS, and optimized the energy allocation strategy of RE suppliers and BSs. Ben Rached N et al [18] adopted two methods for approximating the convex optimization to manage energy purchase strategies under uncertain

energy generation. The proposed algorithm considered energy generation, energy storage and energy sold back to power grids on the precondition that energy requirements of the communication system is satisfied. The authors of [18] also analyzed the benefits generated by the two algorithms for the operators under different energy storage devices but neglected the effect of traffic change, which was due to the positional change in cell users relative to the BS, on BS energy consumption, furthermore, traffic change was an important factor that influences BS energy purchase or allocation strategy. The optimization of energy allocation strategy can effectively reduce system dependence on traditional energies and provide wireless network operators with significant economic benefits, help realize goals of environmental protection and green communication [19], [20].

Most of the existing literatures only consider the energy allocation problem of communication systems from the perspective of energy consumption, which do not consider energy allocation issues in terms of energy consumption, energy storage, energy consumption caused by changes in traffic, and corresponding energy costs. Therefore, a multi-BS collaborative wireless cellular network model under a smart power grid environment was established in the present work. The hybrid energy ratio allocation (HERA) algorithm was proposed based on a comprehensive consideration of the TOU power price of smart power grids, RE generation uncertainty, and BS energy storage. In terms of operator revenue, this algorithm supplies energy to BS systems at a certain ratio of RE and traditional energy on the precondition that system communication quality is guaranteed, thereby effectively lowering the system energy cost.

The remainder of the paper is organized as follows. Section II introduces the system model, including the communication model, power model, and capacity model. Section III presents the idea of the HERA algorithm and the algorithm steps. Section IV presents the simulation parameter settings, simulation results and analysis of the energy distribution using the HERA algorithm. Finally, Section V concludes the paper.

II. SYSTEM MODEL

A. MULTI-BS COLLABORATIVE SYSTEM MODEL

The multi-BS collaborative system model consists of $N(N > 1)$ BSs and is built as illustrated in Fig.1. Each BS is Config-ured with $L(L > 1)$ transmitting antennas and mutually independent RE power generation and energy storage devices. The energy of the BS system is derived from two parts, namely, the power grid and the RE device. The system serves K users, which are recorded as $k = \{1, 2, \dots, K\}$. User positions are randomly distributed within the BS coverage. The present work assumes that no delay occurs in the link post-back between BS and users, and the state information is completely known.

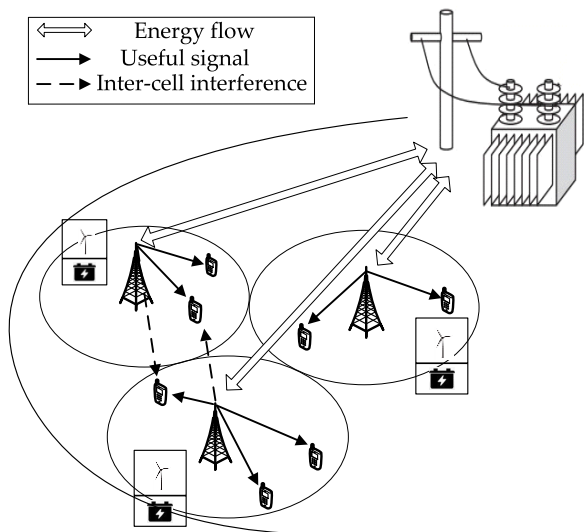


FIGURE 1. System model.

The signal received by user equipment (UE) k in the cell n can be expressed as

$$\begin{aligned}
 y_{n,k} = & \underbrace{h_{n,n,k}x_{n,k}}_{\text{useful signal}} + \underbrace{\sum_{l \in K_n \setminus \{k\}} h_{n,n,k}x_{n,l}}_{\text{UE (same cell) interference}} \\
 & + \underbrace{\sum_{m \in N \setminus \{n\}} \sum_{i=1}^{K_m} h_{m,n,k}x_{m,i}}_{\text{BS (adjacent cell) interference}} + n_{n,k} \quad (1)
 \end{aligned}$$

where $x_{n,k}$ is the pre-coded signal of UE k in the cell n . $h_{n,n,k}$ is the channel vector from UE k in the cell n . $x_{n,l}$ is the pre-coded signal of UE l in the cell n . $h_{m,n,k}$ is the channel vector from BS n to UE k in cell n . K_n is the number of users served by BS n . K_m is the number of users served by BS m ($m \neq n$). $x_{m,i}$ is the pre-coded signal of UE i in the cell n . $n_{n,k}$ is the Gaussian white noise. The first item in Formula (1) is the useful signal received from the BS in this cell. The second item is the multi-user interference from the same cell. The third item is the interference from the adjacent cell.

Assume $h_{n,n,k}, \forall n \in N, k \in K_n$ are already known at the transmitting terminal. ZF pre-coding is used by the transmission channel $\mathbf{H} = [h_{m,n,1}, h_{m,n,2}, \dots, h_{m,n,K_n}]$ to eliminate multi-user interference. The pre-coding matrix is $\mathbf{V} = \mathbf{H}^H (\mathbf{H}\mathbf{H}^H)^{-1}$, which means that $x_{n,k} = v_{n,k}s_{n,k}$ and then $h_{n,n,k}v_{n,l} = 0 (\forall l \in K_n, l \neq k)$. After the precoding, the received signal $y_{n,k}$ and signal-to-noise ratio $SINR_{n,k}$ of UE k in the cell n can be expressed as follows:

$$y_{n,k} = h_{n,n,k}v_{n,k}s_{n,k} + \sum_{m \in N \setminus \{n\}} \sum_{i=1}^{K_m} h_{m,n,k}v_{m,i}s_{m,i} + n_{n,k} \quad (2)$$

TABLE 1. Wind energy generation model simulation setup.

| Wind intensity rank | Weak | Medium | Strong |
|---|---------|---------|---------|
| Probability | P_w | P_m | P_s |
| Generation speed [18] (W/Per time slot) | 300–400 | 400–500 | 600–800 |

$$SINR_{n,k} = \frac{P_n \|h_{n,n,k}v_{n,k}\|^2}{P_m \sum_{m \in N, m \neq n} \sum_{i=1}^{K_n} \|h_{m,n,k}\|^2 \|v_{m,i}\|^2 + \sigma_{n,k}^2} \quad (3)$$

where P_n is the transmitting power of BS n , and P_m is the transmitting power of the BS m ($m \neq n$).

The realizable rate of this user is

$$R_{n,k} = B \log_2(1 + SINR_{n,k}) \quad (4)$$

where B is the bandwidth.

The BS system can be provided with electric energy by a power grid (traditional energy by default) and RE (wind energy). When the electric energy stored by the RE device in the BS has a surplus, the surplus can be purchased back by the power grid. The RE generation cycle is approximately 15 min. Besides, 1 day is divided into $T = 96$ time slots, and the size of each time slot is $\Delta t = 15$ min. The TOU power pricing strategy is adopted by the power grid. Power price is related to power utilization time and is recorded as a_t . The unified power price is adopted for RE and recorded as a_{re} . The price of surplus RE that is purchased back by the power grid is fixed as a_{back} , and $0 < a_{back} < a_t$.

The energy generation velocity of the BS n in the t -th time slots is determined by the wind energy generation model [21],

$$V_{n,t} = \frac{1}{2} \rho A v_u^3 C_p \Delta t \quad (5)$$

where the air density is $\rho = 1.225 \text{ kgm}^{-3}$. The blade swept area is $A = \pi \text{ m}^2$, wind velocity v_u represents the random change in each time slot, and C_p is the conversion coefficient. In previous studies, RE generation is mostly by following statistical data, but the energy generation is more complicated in an actual situation than in the expectation. Therefore, a practical energy generation model is adopted in the present work. Energy is randomly generated in each time slot following the probability of wind strength, as summarized in Table 1. P_w, P_m , and P_s respectively indicate that the power generating device works in the weak wind, medium wind, and strong wind probability, where $P_w + P_m + P_s = 1$, indicating that the probability of weak wind, medium wind, and strong wind is a random value according to the actual weather change. Considering the different positions of BSs and given the actual situation of RE generation, different BSs have various energy generation velocities, that is, $V_{1,t} \neq V_{2,t} \neq \dots \neq V_{n,t}$.

B. SYSTEM POWER CONSUMPTION MODEL

In this work, power consumption mainly includes two parts, namely, the power consumption of all power amplifiers and other circuits. The power consumption of the power amplifiers can be approximated as [22]

$$P_{trans} = \tau P_t \tag{6}$$

where P_t is the transmission power consumption. where P_t is the transmission power consumption. $\tau = \frac{\xi}{\eta}$. ξ is the peak average power ratio. η is the power amplification efficiency of a radio frequency link. τ value is decided by the BS scale and modulation mode.

Circuit loss can be divided into the following two parts [23]: the static power consumption P_{static} and dynamic power consumption. The former is primarily used for the main basic circuit operation of the system, whereas the latter is mainly used for information processing of all nodes. The power consumption of the BS n is

$$P_{n,total} = \kappa P_{trans,n} + P_{static} + \zeta \sum_{n=1}^{K_n} R_{n,k} \tag{7}$$

where κ is the power amplification factor of BS, and ζ is the power consumption of the transmission bit rate per unit.

The total power consumption of BS is

$$P_{total} = \sum_{n=1}^N P_{n,total} \tag{8}$$

The energy loss of each BS in the current time slot is calculated. Specifically, the energy loss of BS n is

$$\Delta E_{n,t} = P_{n,total}^* \Delta t \tag{9}$$

III. MULTI-BS COLLABORATION ENERGY ALLOCATION ALGORITHM

A. SYSTEM ENERGY ALLOCATION PROBLEM

The maximum capacity of the energy storage device equipped for each BS is \bar{C}^0 . The surplus capacity of the energy storage device in the current time lost is $C_{n,t}$. To study the effects of RE and traditional energy hybrid energy supply proportion on the total cost of the system, we assume that the energy consumed by each BS in each time slot is derived from the following two parts: the RE consumption recorded as $L_{n,t}^{re}$ and traditional energy. The energy loss is recorded as $L_{n,t}^{tra}$. The comprehensive power price is the total power price of RE and the traditional energy at a certain power supply ratio. The energy cost (that is, expense generated by energy consumption in this station at the current time slot) of each BS in each time slot is recorded as $Q_{n,t}$ and can be expressed as

$$Q_{n,t} = a_{re} \times L_{n,t}^{re} + a_t \times L_{n,t}^{tra} \tag{10}$$

Given the TOU power pricing strategy in a smart power grid, the energy allocation mode of the BS system will decide its energy cost. Therefore, the HERA algorithm was proposed in this work, which considers the time-of-use price strategy

Algorithm: HERA algorithm

1. Initialize the parameter $E = 0, Q = 0, C_{n,t} = 0$.
2. **for** $t = 1 - 96$ **do**
3. Compute the energy loss $\Delta E_{n,t}$ and power loss $P_{n,total}$ for $\forall n \in N$ using Formulas (7) and (9).
4. **if** a_t is in a low-power-price phase
5. **if** $C_{n,t} \leq \varphi_l, q_t = a_t, L_{n,t}^{re} = 0$, and $L_{n,t}^{tra} = \Delta E_{n,t}$.
6. **else** $q_t = a_t \times \beta_l + a_{re} \times \alpha_l, L_{n,t}^{re} = \Delta E_{n,t} \times \alpha_l, L_{n,t}^{tra} = \Delta E_{n,t} \times \beta_l$.
7. **end if**
8. **else** a_t is in a medium-power-price phase
9. **if** $C_{n,t} \leq \varphi_m, q_t = a_t, L_{n,t}^{re} = 0$, and $L_{n,t}^{tra} = \Delta E_{n,t}$.
10. **else** $q_t = a_t \times \beta_m + a_{re} \times \alpha_m, L_{n,t}^{re} = \Delta E_{n,t} \times \alpha_m, L_{n,t}^{tra} = \Delta E_{n,t} \times \beta_m$.
11. **end if**
12. **else** a_t is in a high-power-price phase
13. **if** $C_{n,t} \geq \bar{C}^0 \times 10\%, q_t = a_{re}, L_{n,t}^{re} = \Delta E_{n,t}, L_{n,t}^{tra} = 0$.
14. **else** $q_t = a_t, L_{n,t}^{re} = 0, L_{n,t}^{tra} = \Delta E_{n,t}$.
15. **end if**
16. **end if**
17. **end for**
18. Compute E and Q using Formulas (17) and (18).

FIGURE 2. HREA algorithm.

based on the traditional priority renewable energy (PRE) algorithm [13]. The energy allocation strategy was regulated in real-time under the TOU power price of the smart power grid. Under low and medium power prices, the strategy with a low RE proportion was adopted for the energy supply to reserve additional RE in the upcoming high-price period. The system energy cost in the whole cycle was lowered by adjusting the energy supply proportion under different power prices.

B. HYBRID ENERGY RATIO ALLOCATION ALGORITHM

Under the TOU power pricing strategy in the smart power grid, the BS system energy allocation mode will decide the system energy cost. The proposed HERA algorithm (see Fig.2) is used to regulate the energy allocation strategy under the TOU power price of the smart power grid. Under low and medium power prices, the strategy with a low RE proportion

was adopted for the energy supply to reserve additional RE in the upcoming high-price period. The system energy cost in the whole cycle was reduced by adjusting the energy supply proportion under different power prices.

The hybrid energy ratio allocation scheme of the HERA algorithm is presented as follows:

If the power price in the current time slot corresponds to the electricity use trough (that is, a low-power-price phase is present), the energy $C_{n,t}$ stored by the BS is smaller than or equal to the lower limit φ_l of energy stored by the BS, and traditional energy is used for power supply, then, $q_t = a_t$, $L_{n,t}^{re} = 0$, and $L_{n,t}^{tra} = 0$. The generated RE is stored in the energy storage device for standby use in the upcoming high-power-price time slot. If the energy stored by the BS exceeds the lower limit φ_l , and the RE of α_l and traditional energy of β_l are adopted, then $q_t = a_t \times \beta_l + a_{re} \times \alpha_l$. The consumption of RE and traditional energy corresponds to

$$L_{n,t}^{re} = \Delta E_{n,t} \times \alpha_l \quad (11)$$

$$L_{n,t}^{tra} = \Delta E_{n,t} \times \beta_l \quad (12)$$

If the power price in the current time slot corresponds to a normal phase (that is, a medium-power-price phase exists), the energy $C_{n,t}$ stored by the BS is smaller or equal to the lower limit φ_m of the energy stored by the BS, and traditional energy is adopted for the power supply, then $q_t = a_t$, $L_{n,t}^{re} = 0$, and $L_{n,t}^{tra} = \Delta E_{n,t}$. At the time, power price is higher than the power price under the aforementioned circumstance, but a high power price may exist in the subsequent time slot. To reduce the total system cost, the generated RE is still stored in the energy storage device for standby use in the high-power-price time slot. If the energy stored by the BS exceeds the lower limit φ_m , then the RE of α_l and traditional energy of β_l are adopted, and $q_t = a_t \times \beta_m + a_{re} \times \alpha_m$. The consumption of RE and traditional energy corresponds to

$$L_{n,t}^{re} = \Delta E_{n,t} \times \alpha_m \quad (13)$$

$$L_{n,t}^{tra} = \Delta E_{n,t} \times \beta_m \quad (14)$$

If the power price in the current time slot corresponds to the peak demand phase for electricity (that is, under a high-power-price phase), and 100% RE is used for energy supply, then $q_t = a_{re}$, $L_{n,t}^{re} = 0$, and $L_{n,t}^{tra} = \Delta E_{n,t}$. However, to guarantee communication quality, when the stored energy is lower than 10% of the BS storage capacity, the system is forced to use traditional energy for power supply and then $q_t = a_t$, $L_{n,t}^{re} = 0$, and $L_{n,t}^{tra} = \Delta E_{n,t}$.

The steps of the HERA algorithm are presented as follows:

Step 1: Initialize the system parameters. In consideration of user mobility feature and random distribution, the RE generation velocity is determined by the probability of weather conditions.

Step 2: Use ZF pre-coding technology to eliminate multi-user interference. Each BS selects users to serve by following the user receiving rate and signal intensity in this cell.

Step 3: Use Formulas (6-9) to calculate the power consumption of each BS in the current time slot.

Step 4: Calculate the energy storage conditions of each BS in the current time slot and fully consider the RE generation velocity and energy consumption in the last time slot.

$$C_{n,t} = C_{n,t-1} + \psi \times V_{n,t} - C_{n,t-1} \times \mu \quad (15)$$

where ψ is the charge rate of the BS energy storage device, and μ is its self-charge rate.

Step 5: Adjust the energy allocation scheme following the power consumption, the energy storage condition in the current time slot, the TOU power price of the smart power grid, and the consumption of RE and traditional energy.

Step 6: Calculate the cost of BS n in the current time slot and the objective function as

$$\Delta Q_{n,t} = q_t \times \Delta E_{n,t} \quad (16)$$

$$\text{s.t. } C_{n,t} \geq \bar{C}^0 \times 10\% \quad (16a)$$

$$0 \leq P_{n,total} \leq P_{\max} \quad (16b)$$

Step 7: At time slot $t = t+1$, if $t \leq T$, then enter the next time slot and return to Step 2. Otherwise, proceed to the next step.

Step 8: Calculate the total energy consumption and total energy cost within a day, respectively, as

$$E = \sum_{t=1}^T \sum_{n=1}^N \Delta E_{n,t} \quad (17)$$

$$Q = \sum_{t=1}^T \sum_{n=1}^N q_t \times \Delta E_{n,t} \quad (18)$$

IV. SIMULATION PARAMETERS AND RESULTS

A. SIMULATION PARAMETERS

For a multi-BS collaborative communication system consisting of $N = 5$ BSs, which are recorded as $n = 1, 2, \dots, 5$, each BS is configured with $L = 4$ transmitting antennas. To adapt to the user motility feature, $K = 20$ single-antenna users are randomly distributed in each time slot within the coverage of the communications system. Table 2 lists the concrete simulation parameters. Without loss of generality, it is assumed here that $P_w = P_m = P_s = 1/3$.

B. SIMULATION RESULTS

Fig.3 displays the energy allocation conditions of the traditional energy supply mode, PRE algorithm, and HERA algorithm, where the traditional energies are used in the traditional energy supply mode, and the PRE and HERA algorithms simultaneously use RE and traditional energy to supply energy to the BS system with an energy storage device. The power grid can purchase back surplus RE to reduce system energy cost. All energies under the traditional energy supply mode come from traditional energy courses. Thus, traditional energy consumption accounts for 100% of the total system energy consumption. Consumptions of RE in the PRE and HERA algorithms account for 23.65% and

TABLE 2. Simulation setup.

| Symbol | Parameter | Assumption |
|--------------|--|-------------|
| P_t | transmission power loss | 40W |
| P_{static} | static power loss | 130W |
| B | band | 8000Hz |
| P_{max} | maximum power consumption | 10kW |
| $SINR_l$ | minimum signal-to-noise ratio requirement | 5dB |
| \bar{C}^0 | maximum capacity of energy storage device | 20kWh |
| ξ | peak average power ratio | 0.1W/bps |
| η | RF link power amplification efficiency | 0.35 |
| ρ | BS power amplification factor | 0.38 |
| ζ | BS power amplification factor | 0.1W/bps/Hz |
| ψ | charging rate of energy storage device | 1w/s |
| μ | self-discharge rate of energy storage device | 0.1% |
| ϕ_l | low electricity price storage energy lower limit | 10kWh |
| α_l | low electricity price consumption RE energy ratio | 0.7 |
| β_l | low electricity price consumption traditional energy ratio | 0.3 |
| ϕ_m | medium electricity price storage energy lower limit | 3kWh |
| α_l | medium electricity prices consumption RE energy ratio | 0.4 |
| β_l | medium electricity prices consumption traditional energy ratio | 0.6 |

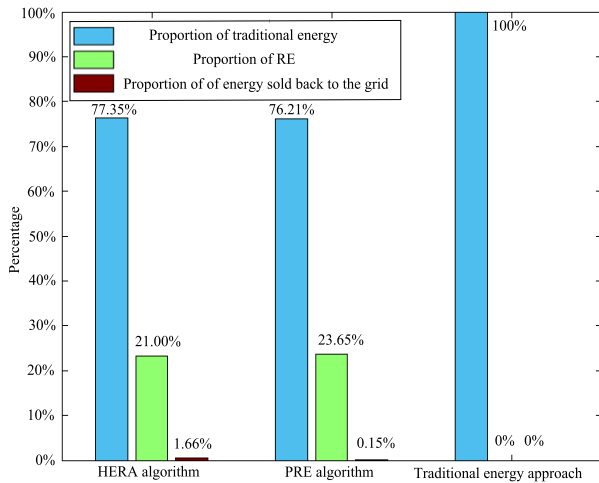


FIGURE 3. Energy distribution under different schemes.

21.00%, respectively. To guarantee system communication quality, the two algorithms have set a lower limit of energy storage, that is, 10%. Priority is given to consuming RE through the PRE algorithm in each time slot. Thus, the system can consume substantial REs, and only 0.15% of the RE in the system is sold back to the power grid. When the HERA algorithm is used, additional REs are stored in the system under low power price until they are used under medium and

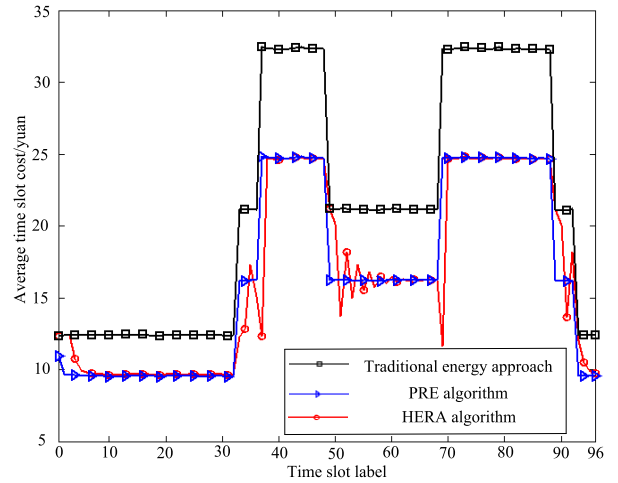


FIGURE 4. Average time slot energy cost under different schemes.

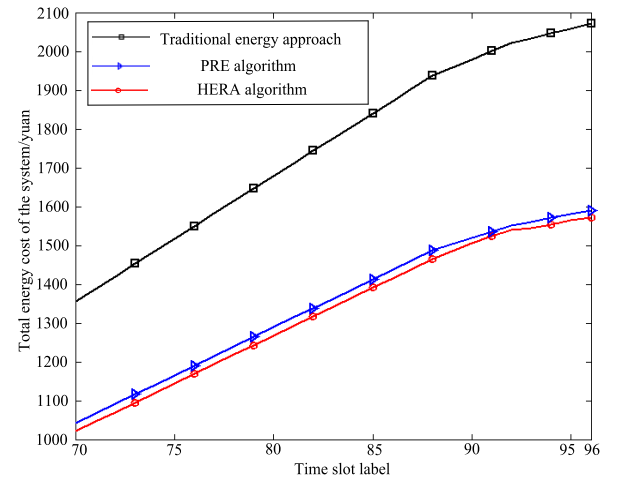


FIGURE 5. Total energy cost of the system under different schemes.

high power prices. Therefore, 1.55% of RE in the system is sold back to the power grid. This part of the profit can be used to reduce the total system energy cost. Therefore, the HERA algorithm uses less RE than the PRE algorithm, but the total system cost is lower in the HERA algorithm than in the PRE algorithm.

Fig. 4 displays the comparison of the average energy costs per time slot under the three allocation schemes. The broken-line graphs for energy cost under the three schemes all vary from TOU power pricing strategies. Energy cost is obviously higher under the traditional energy supply mode than under the power supply mode equipped with the RE energy device because only traditional energies are used under the traditional energy supply mode, and the traditional energy price is higher than the RE price. Power price is low from 0 to the 32nd time slot. The proportional energy supply mode is adopted by the HERA algorithm. Thus, this supply mode will consume more traditional energies than the PRE algorithm. The PRE algorithm has a lower energy cost than the HERA algorithm. From the 32nd to the 40th time slot, power price

TABLE 3. Comparing the energy cost ratio of the system between the HERA and the PRE algorithms under different energy storage lower limits.

| Different energy storage lower limit values under various electricity prices | | Ratio of the HERA algorithm to the energy cost reduction in comparison with that of traditional energy sources | Ratio of the PRE algorithm to the energy cost reduction in comparison with that of the traditional energy supply method | Ratio of the energy cost to the HERA algorithm in comparison with that of the PRE algorithm |
|--|-----------------------------------|--|---|---|
| Low price | Medium price | | | |
| 80% \bar{C}^0 | 60% \bar{C}^0 | 30.48% | 30.29% | 0.19% |
| 80% \bar{C}^0 | 50% \bar{C}^0 | 30.55% | 30.22% | 0.22% |
| 70% \bar{C}^0 | 60% \bar{C}^0 | 30.62% | 30.28% | 0.34% |
| 70% \bar{C}^0 | 50% \bar{C}^0 | 30.61% | 30.26% | 0.35% |
| 60% \bar{C}^0 | 40% \bar{C}^0 | 30.80% | 30.26% | 0.54% |
| 50% \bar{C}^0 | 30% \bar{C}^0 | 30.86% | 30.25% | 0.61% |
| 40% \bar{C}^0 | 30% \bar{C}^0 | 30.66% | 30.30% | 0.35% |
| 30% \bar{C}^0 | 10% \bar{C}^0 | 29.84% | 30.30% | -0.45% |

TABLE 4. Comparing the energy cost ratio of the system between the herA and the PRE algorithms under different energy supply ratios.

| Change in the energy supply ratio under different electricity prices for the same energy storage lower limit value | | | | Ratio of the HERA algorithm to the energy cost reduction in comparison with that of traditional energy sources | Ratio of the PRE algorithm to the energy cost reduction in comparison with that of the traditional energy supply method | Ratio of the energy cost to the HERA algorithm in comparison with that of the PRE algorithm |
|--|------------|------------|------------|--|---|---|
| α_l | β_l | α_m | β_m | | | |
| 0.2 | 0.8 | 0.4 | 0.6 | 30.90% | 30.29% | 0.62% |
| 0.2 | 0.8 | 0.3 | 0.7 | 30.64% | 30.24% | 0.40% |
| 0.3 | 0.7 | 0.4 | 0.6 | 31.20% | 30.25% | 0.95% |
| 0.3 | 0.7 | 0.3 | 0.7 | 31.04% | 30.29% | 0.75% |
| 0.3 | 0.7 | 0.5 | 0.5 | 30.27% | 30.25% | 0.02% |
| 0.4 | 0.6 | 0.4 | 0.6 | 31.40% | 30.28% | 1.12% |
| 0.5 | 0.5 | 0.4 | 0.6 | 31.56% | 30.31% | 1.24% |
| 0.6 | 0.4 | 0.4 | 0.6 | 31.71% | 30.31% | 1.40% |
| 0.7 | 0.3 | 0.4 | 0.6 | 31.74% | 30.28% | 1.46% |
| 0.8 | 0.2 | 0.4 | 0.6 | 31.65% | 30.24% | 1.41% |
| 0.9 | 0.1 | 0.4 | 0.6 | 31.65% | 30.30% | 1.36% |

changes from low to medium and then to high, and the energy storage device in the system can provide additional REs. The energy cost is lower in the HERA algorithm during this time slot than in the PRE algorithm. Fig.5 exhibits the comparison of the total system energy costs under the three schemes. The simulation results indicate that the energy cost per day under the traditional energy supply mode is RMB 2,072.8. The PRE algorithm can reduce such amount by 23.25%, and the HERA algorithm can reduce the amount by 0.19%. The PRE algorithm only concentrates on reducing environmental pollution induced by the communication system, thereby fully exploiting the RE and reducing carbon emission at the maximum. Conversely, the HERA algorithm can reasonably and effectively allocate proportions of RE and traditional energy, balance the improvement of RE utilization efficiency and the reduction of system energy cost, realize the minimum

total energy cost, and reduce the energy cost of network operators.

Fig.6 depicts the HERA algorithm under the condition of TOU power price RE capacity, system energy storage, and system energy consumption changes. The BS energy storage trend and TOU power price change trend are opposite, and the HERA algorithm adopts different proportions of energy supply strategy under different electricity prices, in which low electricity prices use minimal RE. Consequently, energy storage increases. RE also increases with electricity prices. Thus, energy storage decreases, and fluctuations in RE capacity and BS energy consumption also affect energy storage.

To examine the optimal energy distribution ratio, this work further simulates the energy storage lower limit and the ratio of RE to the traditional energy in the HERA algorithm. Table 3 lists the comparison of the HERA and

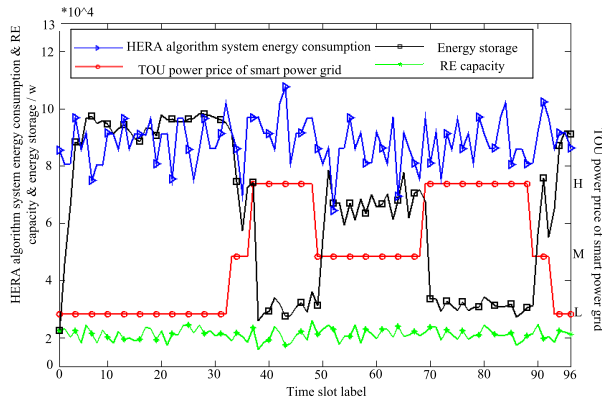


FIGURE 6. System energy consumption of the HERA algorithm under TOU power price, RE capacity, and energy storage changes.

TABLE 5. Comparison of energy costs of different allocation strategies under different wind speed probabilities.

| Different wind speed probabilities | | | Total energy cost under traditional energy supply (RMB) | Total energy cost under the PRE algorithm (RMB) | Total energy cost under the HERA algorithm (RMB) |
|------------------------------------|-------|-------|---|---|--|
| P_w | P_m | P_s | | | |
| 1/2 | 1/4 | 1/4 | 2075.9 | 1623.5 | 1606.6 |
| 1/4 | 1/2 | 1/4 | 2074.0 | 1591.9 | 1574.3 |
| 1/3 | 1/3 | 1/3 | 2071.2 | 1589.8 | 1572.2 |
| 1/4 | 1/4 | 1/2 | 2074.5 | 1562.8 | 1544.7 |

PRE algorithms. In the case of the same energy supply ratio, different energy storage lower limits are compared with the traditional energy supply method to reduce the proportion of system energy cost. In Table 3, when the HERA algorithm at the low price of the energy storage capacity of 50% as the lower limit. The medium electricity price uses 30% of the energy storage capacity as a lower limit and reduces the highest proportion of energy costs in comparison with the PRE algorithm and conventional energy supply. Table 4 presents a comparison of the ratio of the lower energy limit of the stored energy to the same and the different energy supply ratios. The ratio of the HERA and the PRE algorithms to the reduction of the system’s energy cost is also compared with that of the traditional energy supply method (Rows 1–5, Table 4). When the HERA algorithm uses 40% of RE and 60% of traditional energy under medium power price, the algorithm can reduce the energy cost at the maximum relative to the PRE algorithm and traditional energy supply mode. When 70% of the RE and 30% of traditional energy is used under low power price, the HERA algorithm can reduce the energy cost by 31.74% in comparison with the traditional energy supply mode, such amount is 1.46% more than the reduction from the PRE algorithm (Columns 6–11, Table 4).

Table 5 shows the comparison of the total energy costs of the three distribution schemes under different wind speed

probabilities under the optimal energy storage lower limit and energy distribution ratio. It can be seen from the table that the energy cost of the HERA algorithm is always lower than that of the traditional energy supply mode and the PRE algorithm when changing the wind probability P_w , P_m and P_s . Moreover, with the increase of the medium wind probability P_m and the strong wind probability P_s , the energy cost of the HERA algorithm is gradually reduced. The simulation results prove that the HERA algorithm is suitable for energy distribution problems under different wind intensity probabilities, which can effectively reduce the energy cost of the system.

V. CONCLUSION

With the development of RE technology, the hybrid energy supply in smart power grids has increasingly matured. For the energy consumption and energy cost problems of the BS system in the wireless communication network, the proposed HERA algorithm fully considers RE generation uncertainty, TOU power pricing strategy of smart power grids, and BS energy storage. The simulation results indicate that, relative to the traditional energy supply mode and PRE algorithm, the HERA algorithm can reserve more REs under low power price while utilizing more REs under high power price. Thus, the HERA algorithm realizes the lowest energy cost in the whole cycle. The allocation ratio of RE and traditional energy in the hybrid energy ratio algorithm proposed in this work was set as a fixed value. The allocation ratio of and dynamic change in the lower energy storage limit of energy supply strategies will be explored further in a follow-up study.

REFERENCES

- [1] C. A. Chan, W. Li, C.-L. I, A. F. Gygax, C. Leckie, M. Yan, K. Hinton, and S. Bian, “Assessing network energy consumption of mobile applications,” *IEEE Commun. Mag.*, vol. 53, no. 11, pp. 182–191, Nov. 2015.
- [2] M. Kamel, W. Hamouda, and A. Youssef, “Ultra-dense networks: A survey,” *IEEE Commun. Surveys Tuts.*, vol. 18, no. 4, pp. 2522–2545, 4th Quart., 2016.
- [3] X. Ge, S. Tu, G. Mao, and C. X. Wang, “5G ultra-dense cellular networks,” *IEEE Trans. Wireless Commun.*, vol. 23, no. 1, pp. 72–79, Feb. 2016.
- [4] H. A. U. Mustafa, M. A. Imran, M. Z. Shakir, A. Imran, and R. Tafazolli, “Separation framework: An enabler for cooperative and D2D communication for future 5G networks,” *IEEE Commun. Surveys Tuts.*, vol. 18, no. 1, pp. 419–445, 1st Quart., 2016.
- [5] A. Asadi, V. Sciancalepore, and V. Mancuso, “On the efficient utilization of radio resources in extremely dense wireless networks,” *IEEE Commun. Mag.*, vol. 53, no. 1, pp. 126–132, Jan. 2015.
- [6] S. Yang, X. Xu, S. X. Ng, L. Hanzo, and D. Alanis, “Is the low-complexity mobile-relay-aided FFR-DAS capable of outperforming the high-complexity CoMP?” *IEEE Trans. Veh. Technol.*, vol. 65, no. 4, pp. 2154–2169, Apr. 2016.
- [7] Y. Huo, X. Fan, L. Ma, X. Cheng, Z. Tian, and D. Chen, “Secure communications in tiered 5G wireless networks with cooperative jamming,” *IEEE Trans. Wireless Commun.*, vol. 18, no. 6, pp. 3265–3280, Jun. 2019.
- [8] D. Li, G. Zhang, H. Zhao, F. Tian, and Y. Xu, “Integrating distributed grids with green cellular backhaul: From competition to cooperation,” *IEEE Access*, vol. 6, pp. 75798–75812, 2018.
- [9] K. Wang, J. Yu, Y. Yu, Y. Qian, D. Zeng, S. Guo, Y. Xiang, and J. Wu, “A survey on energy Internet: Architecture, approach, and emerging technologies,” *IEEE Syst. J.*, vol. 12, no. 3, pp. 2403–2416, Sep. 2018.
- [10] H. A. H. Hassan, A. Pelov, and L. Nuaymi, “Integrating cellular networks, smart grid, and renewable energy: Analysis, architecture, and challenges,” *IEEE Access*, vol. 3, pp. 2755–2770, 2015.

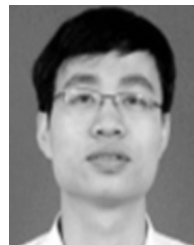
- [11] J. Leithon, T. J. Lim, and S. Sun, "Cost-aware renewable energy management with application in cellular networks," *IEEE Trans. Green Commun. Netw.*, vol. 2, no. 1, pp. 316–326, Mar. 2018.
- [12] Z. Zhu, S. Lambotharan, W. H. Chin, and Z. Fan, "Overview of demand management in smart grid and enabling wireless communication technologies," *IEEE Wireless Commun.*, vol. 19, no. 3, pp. 48–56, Jun. 2012.
- [13] D. Han, B. Zheng, Z. Chen, and S. Li, "Cost efficiency in coordinated multiple-point system based on multi-source power supply," *IEEE Access*, vol. 6, pp. 71994–72001, 2018.
- [14] P. Chakraborty, E. Baeyens, and P. P. Khargonekar, "Cost causation based allocations of costs for market integration of renewable energy," *IEEE Trans. Power Syst.*, vol. 33, no. 1, pp. 70–83, Jan. 2018.
- [15] T. Han and N. Ansari, "Provisioning green energy for base stations in heterogeneous networks," *IEEE Trans. Veh. Technol.*, vol. 65, no. 7, pp. 5439–5448, Jul. 2016.
- [16] G. Ma, G. Xu, Y. Chen, and R. Ju, "Multi-objective optimal configuration method for a standalone wind-solar-battery hybrid power system," *IET Renew. Power Gener.*, vol. 11, no. 1, pp. 194–202, Nov. 2017.
- [17] D. Li, W. Saad, I. Guvenc, A. Mehbodniya, and F. Adachi, "Decentralized energy allocation for wireless networks with renewable energy powered base stations," *IEEE Trans. Commun.*, vol. 63, no. 6, pp. 2126–2142, Jun. 2015.
- [18] N. Ben Rached, H. Ghazzai, M.-S. Alouini, and A. Kadri, "Energy management optimization for cellular networks under renewable energy generation uncertainty," *IEEE Trans. Green Commun. Netw.*, vol. 1, no. 2, pp. 158–166, Jun. 2017.
- [19] H. Ghazzai, E. Yaacoub, M.-S. Alouini, and A. Abu-Dayya, "Optimized smart grid energy procurement for LTE networks using evolutionary algorithms," *IEEE Trans. Veh. Technol.*, vol. 63, no. 9, pp. 4508–4519, Nov. 2014.
- [20] D. S. Han, B. Zheng, and Z. Chen, "Sleep mechanism of base station based on minimum energy cost," *Wireless Commun. Mobile Comput.*, vol. 2018, Mar. 2018, Art. no. 4202748. doi: [10.1155/2018/4202748](https://doi.org/10.1155/2018/4202748).
- [21] Z. Lin, Z. Chen, S. Yang, H. Meng, and Q. Wu, "Coordinated pitch & torque control of large-scale wind turbine based on Pareto efficiency analysis," *Energy*, vol. 147, pp. 812–825, Mar. 2018.
- [22] C. Isheden and G. P. Fettweis, "Energy-efficient multi-carrier link adaptation with sum rate-dependent circuit power," in *Proc. IEEE Global Telecommun. Conf.*, Dec. 2010, pp. 6–10.
- [23] S. Bu, F. R. Yu, Y. Cai, and X. P. Liu, "When the smart grid meets energy-efficient communications: Green wireless cellular networks powered by the smart grid," *IEEE Trans. Wireless Commun.*, vol. 11, no. 8, pp. 3014–3024, Aug. 2012.



DONGSHENG HAN was born in Qiqihar, China, in 1980. He received the B.Eng. degree in telecommunications engineering from North China Electric Power University, China, in 2003, and the Ph.D. degree in communication and information systems from Beijing Jiaotong University, China, in 2012. He is currently an Associate Professor with the School of Electrical and Electronic Engineering, North China Electric Power University. His main research interests include digital communication systems and wireless communication.



SHIJIE LI was born in Qinhuangdao, China, in 1993. He received the B.S. degree in electronic information engineering from the North China Institute of Aerospace Engineering, China, in 2017. He is currently pursuing the M.S. degree in electrical and electronic engineering with North China Electric Power University. His main research interests include digital communication systems and wireless communication.



ZHIXIONG CHEN was born in Putian, China, in 1983. He received the master's degree in communication and information systems from the Harbin Institute of Technology, China, in 2007, and the Ph.D. degree in electrical engineering and its automation from North China Electric Power University, China, in 2010, where he has been a Lecturer with the School of Electrical and Electronic Engineering, since 2010. His main research interests include channel coding and power system communication.

• • •